Hypertension Research (2018) 41:506–514
https://doi.org/10.1038/s41440-018-0045-1

ARTICLE

Stromal interaction molecule 1 modulates blood pressure via NO production in vascular endothelial cells

Mitsuhiro Nishimoto[1,2,3] · Risuke Mizuno[1,3] · Toshiro Fujita[2,3] · Masashi Isshiki[1,4]

Received: 4 December 2017 / Revised: 8 January 2018 / Accepted: 14 January 2018 / Published online: 25 April 2018
© The Japanese Society of Hypertension 2018

Abstract

In vascular endothelial cells, store-operated calcium entry (SOCE) activates endothelial NO synthase (eNOS) and regulates nitric oxide (NO) production as well as flow-dependent mechanical stimuli. Stromal interaction molecule 1, or STIM1, was recently identified to be essential for SOCE, acting as a calcium sensor for intracellular calcium stores. However, how STIM1 affects endothelial function and blood pressure (BP) remains unclear. We generated STIM1 *fl/fl* mice and vascular endothelial cell-specific STIM1 knockout mice using the Cre–loxP system, and conducted experiments using these mice to clarify the physiological role of STIM1 in vascular endothelial function and BP as follows: (1) SOCE was analyzed in isolated aortic endothelial cells by calcium add-back with fluorescent Ca^{2+} indicators. Phosphorylation of eNOS and NO production were evaluated by immunoblotting and the NO indicator, respectively. (2) Tension of aortic rings was measured in 10-week-old mice in response to acetylcholine. (3) BP was measured in 10-week-old mice by the telemetry system. The results were: (1) SOCE, eNOS activation, and NO production were suppressed by ~50–60% in endothelial cells from STIM1 knockout. (2) Endothelium-dependent vasodilation was decreased in aortic rings from STIM1 knockout mice, whereas endothelium-independent relaxation was not altered. (3) STIM1 knockout mice exhibited significant BP elevation, especially in nighttime. ($124.3 \pm 2.5/99.2 \pm 3.9$ vs. $114.1 \pm 3.2/83.6 \pm 1.7$ (nighttime, mmHg), $109.7 \pm 1.7/83.0 \pm 3.0$ vs. $104.8 \pm 3.3/73.7 \pm 1.6$ (daytime, mmHg), knockout vs. control, respectively). In conclusion, STIM1 in vascular endothelial cell modulates vascular function through NO production and has a major role in regulating BP, especially in the active time.

Introduction

Hypertension is one of the most important cardiovascular risk factors leading to atherosclerosis, stroke, ischemic heart disease, and renal dysfunction [1]. The mechanism of blood pressure (BP) regulation is complex and remains not fully clarified; however, dysregulation of vascular function profoundly contributes to the elevation of BP [2, 3]. Vascular endothelial cells (ECs) do not only form the inner surface layer of blood vessels, but play a pivotal role in regulating diverse biological functions through secreting various vasoactive factors [4, 5]. Among these factors, nitric oxide (NO) is a strong vasodilator and tightly modulates vascular function, including BP regulation. Under physiological conditions, NO is mainly produced by endothelial NO synthase (eNOS) in ECs [6], and previous reports have already shown that both genetic and pharmacological ablation of eNOS induces significant BP elevation [7–9], indicating its impact on vascular function. The activity of eNOS is regulated by various factors and stimuli including Ca^{2+}-bound calmodulin, phosphorylation, co-factors, and intracellular sublocations [10, 11]. Among such contributors of eNOS activity, the intracellular ionized-calcium concentration ($[Ca^{2+}]_i$) is fast and critically important one.

Intracellular free calcium ions are ubiquitous second messengers for various cell functions. They have two major

Electronic supplementary material The online version of this article (https://doi.org/10.1038/s41440-018-0045-1) contains supplementary material, which is available to authorized users.

✉ Masashi Isshiki
isshikim@saitama-med.ac.jp

[1] Department of Molecular Vascular Endocrinology, Graduate School of Medicine, Tokyo, Japan

[2] Department of Nephrology and Endocrinology, Faculty of Medicine, Tokyo, Japan

[3] Division of Clinical Epigenetics, Research Center for Advanced Science and Technology, The University of Tokyo, Tokyo, Japan

[4] Department of Endocrinology and Diabetes, School of Medicine, Saitama Medical University, Saitama, Japan

sources; one is intracellular calcium stores, the majority of which is thought to be in the endoplasmic reticulum (ER), and the other is influx from the extracellular space. In non-excitable cells including vascular ECs, store-operated calcium entry (SOCE) is important to initiate critical physiological responses [12]. The stimulations activating phospholipase C lead to the production of IP_3, which mobilizes calcium from ER Ca^{2+} stores, and calcium depletion in the ER induces calcium influx from the extracellular space. This influx is called SOCE. Because most eNOS is located directly beneath the plasma membrane, SOCE is more potent in activating eNOS than calcium release from intracellular stores in vascular ECs [13].

Shear stress and G-protein coupling receptor (GPCR)-agonists including ATP and bradykinin are two known major stimulator of eNOS in vivo. GPCR agonists activate eNOS mainly through SOCE. On the other hand, shear stress activates eNOS through calcium-independent [14] and calcium-dependent pathway distinct from GPCR/SOCE [15] or involving GPCR/SOCE pathway [16, 17]. The contribution of each pathway to the vascular function in vivo is to be elucidated.

Stromal interaction molecule 1 (STIM1) was identified as an essential mediator of SOCE, acting as a calcium sensor for intracellular calcium stores [18]. STIM1 has been shown to mediate SOCE in various types of tissues including vascular endothelium. STIM2 is the only known homolog of STIM1 and has highly similar structure with STIM1, including a calcium-binding domain and an ER-locating signal peptide, and coiled-coil domains with a conserved structure in the cytoplasmic region [19]. STIM2 evokes only minimal SOCE by detecting small decreases of calcium concentration in ER because of its lower affinity to calcium ions than STIM1 [20]. Thus, STIM2 is speculated to play some roles in maintaining calcium concentration of cytosol and ER [20, 21]. STIM2 is also reported to compensate SOCE in several tissues depending on its expressing ratio with STIM1. For example, STIM2 plays a relatively large role in neurons [22, 23], whereas STIM1 is prominent, in other tissues such as immune cells [24]. In ECs, there are few evidences showing the contribution of STIM2 to SOCE. In an in vitro study, STIM1 plays an important role in EC proliferation [25] and affects NO-mediated vascular permeability by thrombin, which evokes both SOCE and receptor-operated calcium entry [26]. In the rodent models, endothelial STIM1 reportedly modulates vascular permeability during inflammation [27]. In addition to these physiological functions, STIM1 was also reported as a potential pathological modulator. In an atherosclerotic-prone type 1 diabetic mouse model, STIM1 expression is reduced in coronary endothelium, leading to vascular dysfunction, which can be rescued by STIM1 overexpression [28]. Thus, the suppression of STIM1 in ECs may contribute to progression of diabetes-associated atherosclerosis. We supposed measuring and analyzing the BP profile of EC-specific STIM1-deficient mice may clarify the role of endothelial STIM1 and SOCE on endothelial function and BP regulation, additionally, support to understanding the distinguishable role of agonist-induced modulation on vascular function and BP control from the flow-mediated ones. Recently, EC-specific STIM1-deficient mice exhibit no BP elevation measured by a tail-cuff method despite of the impaired endothelial function [29]. However, the measuring method was not sufficient to evaluate precise BP. Thus. BP was more precisely and continuously measured by the radio-telemetry system in this study.

Methods

Materials and methods are described in detail in the online supplement.

Generation of vascular endothelial cell-specific STIM1 KO mice

Animal experiments conformed the National Institutes of Health guidelines, Guide for the care and use of laboratory animals and the protocols were approved by the Experimental Animal Research Committee at the University of Tokyo (permission #P10–065). STIM1 floxed mice (Flox) were commercially developed by UNITECH Co., Ltd. (Chiba, Japan) as a custom order. The STIM1 conditional gene-targeting vector was electroporated into C57B/6 J ES cells. One positive ES clone was used for implantation and obtained chimeras with targeted events (with Neo^{frt}/$STIM1^{flox}$ allele) were crossed with Tg-FLP mice to remove the Neo cassette. The mice harboring the $STIM1^{flox}$ allele were backcrossed to C57BL/6 J mice to remove the FLP gene and then crossed with C57BL/6 J Tie2-Cre mice (UNITECH Co., Ltd., Chiba, Japan), in which the Cre recombinase was driven by the Tie2 promoter, which is active in entire vascular ECs [30]. Information regarding the generation of EC-specific STIM1 knockout (ECKO) mice is illustrated in Fig. S1A.

All experiments were conducted in 10–12-week-old male mice, but isolation of ECs was conducted in 6-week-old male mice. Flox were used as a control. Numbers of animals used for each experiment are shown in figures.

Cell culture

Aortic ECs were isolated from 6-week-old male mice by a modified method as previously described [31]. In brief, mice were killed by exsanguination under isoflurane

anesthesia (2–2.5%) and aortas were obtained immediately. After immediate removal of connective tissues, aortas were filled with collagenase type II and incubated for 45 min. ECs were obtained from aortas by flushing. To remove smooth muscle cells, after 2 h incubation at 37 °C on type I collagen-coated dishes, the medium was replaced by growth factor-enriched medium. One week later, 35 mm-subconfluent ECs were obtained. More than 95% of obtained cells were CD31-positive and showed AcLDL uptake (Fig. S2).

Immunoblotting

Tissue or cultured cells were lysed in radio immunoprecipitation assay buffer (50 mmol/L Tris-HCl (pH7.4), 150 mmol/L NaCl, 1% (v/v) IGEPAL CA630, 1% (w/v) sodium deoxycholate, 0.1% (w/v) sodium dodecyl sulfate) with protease inhibitors and 1 mmol/L NaF. Laemmle's sample buffer was added to the samples, which were then subjected to sodium dodecyl sulfate polyacrylamide gel electrophoresis. The proteins were transferred onto a polyvinylidene difluoride membrane. After incubation with the indicated primary antibodies, the membranes were incubated with horseradish peroxidase-conjugated secondary antibodies. The immunoreactive bands were visualized using ImmunoStar LD (Wako), and detected with a LAS4000mini (GE Healthcare, USA). The density of the bands was quantified by ImageJ 1.47 g (Wayne Rasband, NIH, USA).

Ca^{2+} measurements

Cells were loaded with the fluorescent calcium indicator Fluo 4-AM and Fura Red AM as previously described [32] and $[Ca^{2+}]_i$ was measured by analyzing fluorescence intensity with a Leica confocal microscopy system TCS SP2 equipped with an Ar laser and an HCX PL APO 40.0 × 1.25 OIL objective (Leica microsystems K.K., Tokyo, Japan). Cells were excited at 488 nm and images of emissions ranging from 500–540 nm (F_{Fluo4}) and 600–680 nm ($F_{FuraRed}$) were simultaneously obtained. SOCE was recorded as the calcium influx induced by 1×10^{-3} mol/L calcium chloride administration after a 10 min incubation of 5×10^{-6} mol/L thapsigargin (calcium add-back method). The maximum reaction occurred with the calcium ionosphere, ionomycin (10^{-6} mol/L). The index F was calculated as the ratio of F_{Fluo4} to $F_{FuraRed}$, and corrected by F_{max} as the maximal response and F_0 as the initial intensity. $[Ca^{2+}]_i$ was presented as $F/(F_{max} - F_0)$.

NO measurements

ECs were isolated from three mice of each genotype into independent dishes, and each dish was divided into three preparations. ECs were co-incubated overnight with Piccells, cell lines expressing a fluorescent resonance energy transfer-based NO sensor [33] (a kind gift from Dr. Moritoshi Sato, the University of Tokyo, Tokyo, Japan). The ratio of Piccells to ECs at the beginning of culture was ~1:10. The culture medium was replaced with calcium-free Hank's balanced salt solution and images were obtained using the TCS SP2 confocal microscopy system with a × 40 objective. One-third to half of the scanning field was covered by Piccells owing to the difference in proliferation rate between ECs and Piccells. All Piccells in the field of view were excited at 442 nm. Fluorescence images were obtained at 467–497 nm for cyan fluorescent protein (F_C) and at 508–543 nm for yellow fluorescent protein (F_Y). The fluorescence ratio R was calculated as F_Y/F_C and R_0 was defined as the average of R for 1 min of incubation before administration of thapsigargin. The results of NO production were presented as the ratio R/R_0 and quantified by an area under the curve (AUC) above 1.0. An AUC from 0 to 15 min after thapsigargin administration was designated as the first peak and the area at 15–20 min (0–5 min after calcium add-back) was the second peak.

Isometric force measurements

Isometric force measurements were performed as described previously [32]. Ten-week-old mice were killed by collection of whole blood under isoflurane anesthesia (2–2.5%) and the aortas were immediately obtained and stripped of connective tissue. The endothelium was not removed. The aorta was cut transversally in ring segments. The preparation was performed in Krebs solution (112 mmol/L NaCl, 25.2 mmol/L $NaHCO_3$, 4.73 mmol/L KCl, 1.19 mmol/L $MgCl_2$, 1.19 mmol/L KH_2PO_4, 0.9 mmol/L $CaCl_2$, 0.026 mmol/L ethylenediaminetetraacetate disodium, and 11.0 mmol/L glucose), aerated with a mixture of 95% (v/v) O_2 and 5% (v/v) CO_2. The vascular rings were mounted between two tungsten wires, in a 37 °C-water-circulating tissue bath. One wire was stationary, whereas the other was connected to a force transducer (TB-651T; Nihon Kohden Corp., Tokyo, Japan). The rings were equilibrated with a resting force of 2 g for 30 min, contraction by 60 mM KCl was measured twice with 30 min interval. After 30 min incubation, cumulative application of phenylephrine (PE) (1×10^{-10} –1×10^{-5} mol/L) was conducted. The medium was exchanged three times, then vehicle or 1×10^{-4} mol/L L-NAME was added to media. After 20 min incubation, the rings were contracted with submaximal concentration of phenylephrine (10^{-6} mol/L) and when the contractile response reached a plateau, cumulative application of acetylcholine (ACh) (1×10^{-10} –1×10^{-5} mol/L) was initiated to examine endothelium-dependent reactions. To examine endothelium-independent reactions of smooth

muscle cells, sodium nitroprusside (SNP) was also applied cumulatively (1×10^{-10}–1×10^{-5} mol/L). Contraction induced by PE was presented as a percentage of maximal contraction of KCl and relaxations by ACh and SNP were presented as a percentage of the initial tension.

BP measurements by radio-telemetry

BP of conscious mice were measured with an implantable BP transmitter (TA11PA-C10), RPC-1 receiver, APR-1 ambient pressure monitor, and a Data Quest ART Silver 2.3 acquisition system (Data Sciences International, St. Paul, MN), as previously described [34]. Mice were anesthetized with isoflurane and the transmitter catheter was inserted into the left common carotid artery, and the transmitter was placed in a subcutaneous space of the right trunk. Mice had access to normal chow and water *ad libitum* for the duration of the study. Recording began after a recovery period of 7–10 days. In order to compare the circadian variation of BP, we performed fitting to sinusoidal curve in a linear regression to calculate an amplitude of the sinusoidal wave for each mouse by R (R Core Team (2016). R: A language and environment for statistical computing. R Foundation for Statistical Computing, Vienna, Austria. URL https://www.R-project.org/). Mice in the breeding room were maintained on a 12-h light–dark cycle. BP and heart rate were measured for 15 s every 60 min for 3 days.

Statistical analyses

Data are expressed as the mean ± SEM and analyzed by R version 3.2.4. Comparison of mean values between the two groups was performed by Wilcoxon's rank sum test and comparison of mean values between multiple groups was performed by Tukey's honest significant difference test. $P < 0.05$ was considered to be statistically significant.

Results

STIM1 deletion reduces SOCE in vascular ECs

ECKO looked normal and proved to be fertile. They showed no differences, when compared with floxed mice (Flox), in body weight (24.4 ± 0.9 g, $n = 14$, vs. 24.0 ± 0.3 g, $n = 20$, Flox vs. ECKO, respectively), kidney weight (148.9 ± 4.6 mg, $n = 4$ vs. 144.9 ± 8.9 mg, $n = 6$), or heart weight (106.6 ± 1.9 mg, $n = 4$, vs. 106.4 ± 3.2 mg, $n = 6$). The ablation of STIM1 in vascular ECs was confirmed by quantitative reverse transcription-polymerase chain reaction, immunoblotting of isolated vascular ECs, and immunofluorescence of excised aortic tissues (Fig. S1B, C, D). The null allele was detected in various tissues at different expression level (Fig. S1E). Among them, endothelium-rich lung and heart demonstrated relatively higher expression, reflected by successful KO specifically in ECs. Vascular smooth muscle cells (VSMCs) exhibited no morphological changes such as aortic media thickness or periarterial fibrosis in ECKO aortas (Fig. S1D, S3). The expression of STIM1 in VSMC was not different between Flox and ECKO mice (Fig. S1D). STIM2 is the only homologue of STIM1 and also regulates calcium influx depending on ER calcium stores, but mainly works on basal calcium homeostasis [20]. Although STIM2 was reported to compensate for the function of STIM1 to some extent, the expression of STIM2 was not affected by STIM1 ablation in several types of cells [35, 36]. Consistently, the expression of STIM2 was not altered in isolated ECs in our model (Fig. S1B).

To evaluate SOCE, the cells were incubated in Ca^{2+}-containing recording medium, following the treatment with thapsigargin, a sarco/ER Ca^{2+}-ATPase inhibitor, in the absence of extracellular Ca^{2+}. $[Ca^{2+}]_i$ elevation in SOCE was dramatically blunted in ECs from ECKO (0.12 ± 0.01, $n = 3$) when compared with Flox (0.38 ± 0.03, $n = 3$) (Fig. 1). Although STIM2 was also expressed in isolated vascular ECs (Fig. S1A, B), the effect of STIM1 ablation on SOCE was prominent, suggesting that STIM2 cannot compensate for STIM1 deletion in this model.

STIM1 modulates eNOS activation and NO production in vascular ECs

In ECs from ECKO, calcium add-back-induced eNOS phosphorylation at serine 1177 was significantly attenuated (Flox vs. ECKO, 11.6 ± 0.38 vs. 6.2 ± 0.44, $n = 3$, respectively) (Fig. 2*A*, *B*). Similarly, NO production induced by

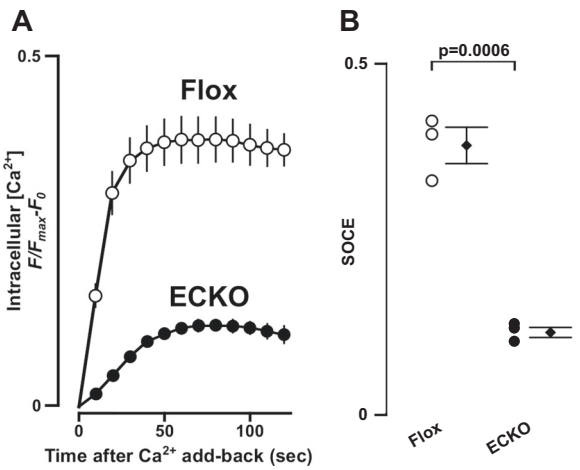

Fig. 1 Store-operated calcium entry in isolated aortic endothelial cells. *A* Traces of the $[Ca^{2+}]_i$ changes of isolated ECs recorded by fluorescence intensity. $[Ca^{2+}]_i$ changes were shown after calcium add-back. ***B*** Quantification of SOCE corrected by the maximum reaction obtained by ionomycin treatment. Error bars represent S.E.M. ($n = 3$)

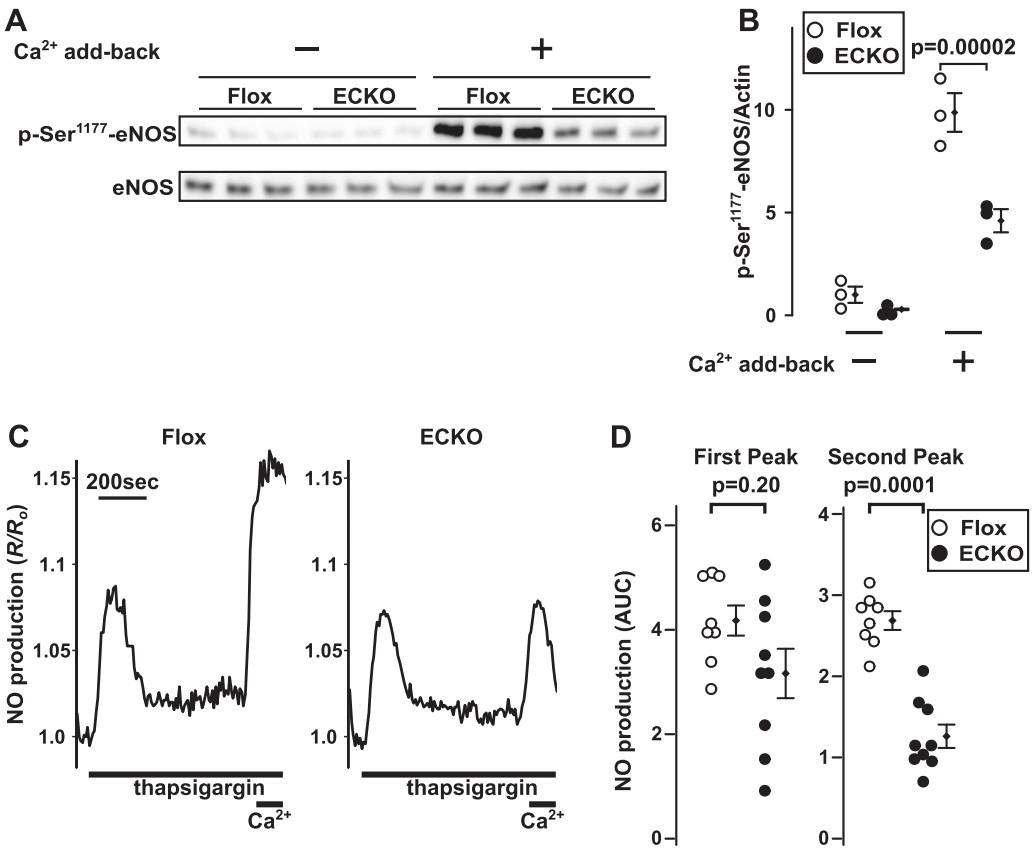

Fig. 2 eNOS activation and NO production induced by SOCE in isolated aortic ECs. ***A*** Representative immunoblotting for eNOS phosphorylation at Ser1177 and total eNOS with or without SOCE by calcium add-back. ***B*** Quantification of densitometry analysis of Fig. 2*A*. ***C*** The representative traces for NO production in isolated ECs induced by calcium add-back; the AUC from 0 min (the start of thapsigargin) to 15 min (calcium add-back) was calculated as the first peak and the one from 15 min to 20 min as the second peak in Fig. 2*D*. ***D*** Quantification of the AUC of NO production. The first peak indicates NO production by calcium release from intracellular stores, and the second by calcium influx from the extracellular space. Flox:$n = 8$, ECKO:$n = 9$, Error bars represent S.E.M

SOCE (second peak in Fig. 2*C*, *D*, S4), was significantly reduced in cells from ECKO (1.30 ± 0.15, $n = 9$, Fig. 2*D*, S4) when compared with the cells from Flox mice (2.67 ± 0.16, $n = 8$, Fig. 2d, S4). In contrast, the first peak, which indicates NO production induced by calcium release from intracellular stores, was not different between the two strains (Flox vs. ECKO, 3.16 ± 0.47 vs. 3.76 ± 0.56, respectively, $p = 0.34$, Fig. 2c, d, S4).

Deletion of STIM1 enhances aortic contraction and attenuates EC-dependent relaxation

We explored the vascular function by the aortic rings. PE-induced contractions were significantly enhanced in aortic rings from ECKO ($n = 30$) compared with Flox ($n = 20$) (Fig. 3A). ACh-induced relaxation was significantly attenuated in ECKO ($n = 10$) than those from Flox ($n = 6$) (Fig. 3B). L-NAME, an eNOS inhibitor, completely inhibited ACh-mediated relaxation (Fig. 3B), indicating that relaxation was due to eNOS activation. In contrast, relaxation of rings by SNP, an NO donor, was not different between the two groups (Fig. 3C). Thus, STIM1 deletion in ECs induced enhanced contraction induced by α-adrenergic stimulation, and specifically abrogated endothelium-dependent vascular relaxation, not affecting endothelium-independent reactivity of VSMC.

Vascular endothelial cell-specific STIM1 deletion mice exhibit BP elevation

BP measured by the radio-telemetry system showed that ECKO exhibited significant systolic BP (SBP) elevation during the nighttime and diastolic BP (DBP) elevation during the daytime and nighttime (Fig. 4A, B). Daytime SBP exhibited the same pattern; however, the difference was not statistically significant (109.7 ± 1.7 mmHg vs. 104.8 ± 3.3 mmHg, ECKO ($n = 5$) vs. Flox ($n = 5$), respectively, $p = 0.3$) (Fig. 4A, B). As a result, the circadian variations of both SBP and DBP in ECKO were significantly larger than those in Flox (8.9 ± 0.4 vs. 6.1 ± 0.6 mmHg in SBP ($p = 0.008$), 10.3 ± 0.5 vs. 6.1 ± 0.4 mmHg in DBP ($p = 0.008$), ECKO ($n = 5$) vs. Flox ($n = 5$),

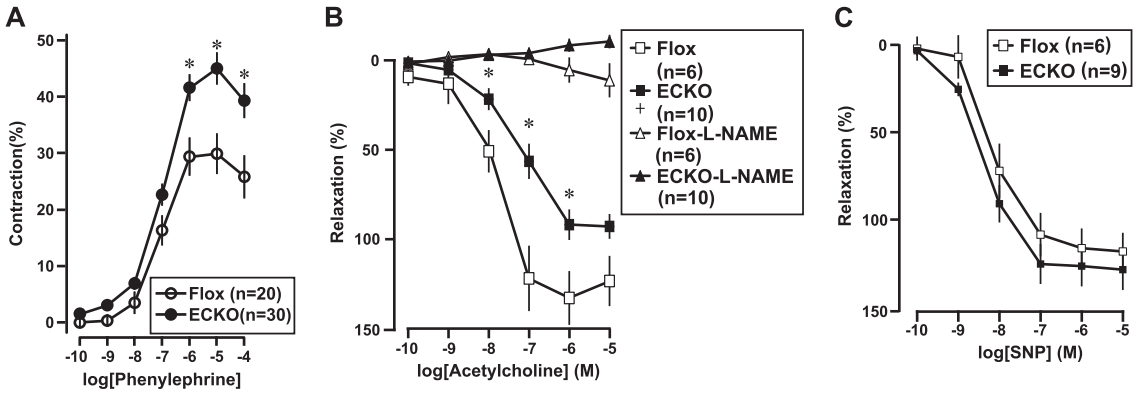

Fig. 3 Vascular function in aortic rings of Flox and ECKO. Dose-dependent contraction induced by phenylephrine ***(A)*** of aorta from Flox ($n = 20$) and ECKO ($n = 30$). PE-induced contraction was expressed as a percentage of contraction by KCl. Dose-dependent relaxation induced by acetylcholine with or without L-NAME (***B***) and sodium nitroprusside (***C***). Error bars represents S.E.M. *: $p < 0.05$ vs. Flox

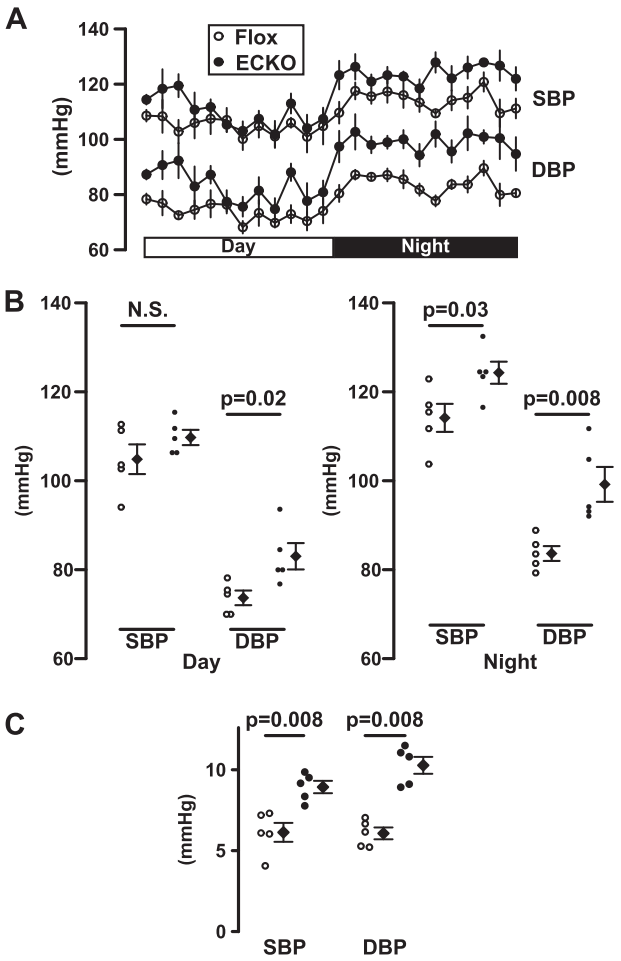

Fig. 4 Blood pressure of Flox and ECKO mice. ***A*** The circadian change of the blood pressure of Flox and ECKO measured by telemetry. ***B*** Daytime blood pressure (Day, average of blood pressure during 9 to 20 h), and nighttime blood pressure (Night, average of blood pressure during 21 to 8 h). ***C*** Amplitude of fitted sinusoidal curve calculated from BP plot for 3 days in each mouse. $n = 5$, SBP: systolic blood pressure, DBP: diastolic blood pressure

respectively) (Fig. 4C). Heart rate did not differ significantly between the two strains during the daytime (466 ± 29 bpm vs. 531 ± 26 bpm, Flox vs. ECKO, $p = 0.10$) nor nighttime (508 ± 24 bpm vs. 575 ± 20 bpm, $p = 0.06$).

Discussion

In this study, we first confirmed by in vitro and ex vivo study that STIM1 expression affects SOCE, eNOS activation, NO production, and endothelial function. Most importantly, we found for the first time that endothelial STIM1 regulates BP. The elevation of BP in EC-specific STIM1-deficient mice had several features; milder phenotype than eNOS-deficient mice, nighttime-dominant, and diastolic-dominant.

Two previous reports focused on STIM1 of ECs in vivo models. Gandhirajan et al. reported EC-specific STIM1-deficient mice, using another EC-specific promoter-fused Cre recombinase expression system. They demonstrated that ablation of STIM1 in ECs decreased the permeability of lung vascular endothelium in acute inflammation. However, it is not clear how STIM1 functions in the systemic vasculature and in chronic vascular inflammation [27]. Recently, Kassan et al. also reported EC-specific STIM1-deficient mouse model harboring the *Cre* transgene driven by an identical promoter to ours. Mice exhibited attenuated vascular relaxation through deficiency of the NO–cyclic GMP pathway, consistent with our results [29]. However, their mouse model did not exhibit any BP elevation. We speculate several reasons for this critical discrepancy, some of which include differences in age and the method for BP measurement. In their study, only daytime systolic BP was measured in mice 1–2 weeks younger than ours. Ageing generally accelerates BP elevation. In addition, the exact

method of BP measurement was not clearly stated in their report [29]; however, the tail-cuff method was most likely used given that single values of SBP for each genotype were described. The tail-cuff method has several limitations; BP is indirectly measured in the restrained conditions. Telemetry used in this study enabled us to directly and continuously measure BP in non-stressed-free conditions. Therefore, we can evaluate BP much more precisely than BP measured by tail-cuff method.

In addition to the attenuated vaso-relaxation response to ACh, our mice exhibited the enhanced contraction induced by PE (Fig. 3). Although apparent morphorlogical differences were not detected in VSMC of aorta (Fig. S3), STIM1 ablation in ECs functionally altered the contractile profile of VSMC. Because responses to SNP were not different, the sensitivity of VSMC to NO was not altered. Taken together, not only direct vasoconstriction induced by NO deficiency but also enhanced vasoconstriction induced by α adrenergic stimulation contributes to the development of hypertension in ECKO. This speculation is supported by the present finding that elevation of nighttime BP was apparently greater than that of daytime BP in ECKO (Fig. 4), although we did not evaluate sympathetic activity. Given that plasma NE concentration is higher during the active phase than during the inactive phase, ECKO-induced augmentation of vasoconstrictive response to PE might lead to the significant BP difference between ECKO and Flox during the active phase but not during inactive phase.

STIM1 ablation in ECs induced BP elevation by impairing NO production, as we expected. However, compared with eNOS knockout mice and L-NAME-infusion mice [9], BP elevation in our model was relatively small, although both NO production and ACh-induced vasodilation in ECKO are suppressed to a similar extent as those of eNOS knockout mice [37]. One factor accounting for the milder phenotype of ECKO as compared to other eNOS-deficient model mice may be that Ca^{2+} release from the intracellular calcium store remains intact and results in maintaining NO production (Fig. 2). Alternatively, shear stress in vivo profoundly activates eNOS in ECKO. Given that a certain fraction of Ca^{2+} influx evoked by shear stress is receptor-operated and distinct from SOCE [15], it should be noted that addition of calcium-containing medium in calcium add-back procedure in vitro may cause mechanical stress and subsequently even small amount of Ca^{2+} influx can induce NO production owing to the neighboring location of eNOS in plasmalemmal caveolae as we previously reported [38].

BP elevation was relatively small in the systolic phase as compared to the diastolic phase, and was associated without apparent cardiac hypertrophy at 10 weeks old, because heart weight is less influenced by DBP than SBP [39]. Isolated diastolic hypertension (IDH) is prevalent clinically, especially in the young [40, 41] the obese [42] and individuals with obstructive sleep apnea syndrome [43], and can be a predictor of future systolic and diastolic hypertension [44]. A cohort of ENIGMA study subjects has shown that the major hemodynamic abnormality underlying IDH comes from increased peripheral vascular resistance, not cardiac output or aortic stiffness, whereas isolated systolic hypertension patients showed decreased peripheral vascular resistance compared with normotensive subjects [45]. Therefore, endothelial dysfunction may predominantly induce peripheral vasoconstriction, resulting in elevated BP in the diastolic phase. In addition to the important role in regulating vascular tone, NO in the kidney, partially produced by eNOS, inhibits sodium re-absorption [46] and eNOS knockout mice exhibit salt-sensitive hypertension [9, 47]. Thus, further studies focusing on the function of STIM1 in ECs of the kidney are required, especially with respect to salt-sensitive hypertension.

Another feature of BP elevation of our ECKO mice was nighttime-dominance, resulting in the larger circadian variation. BP elevation in active phase is associated with psycological stress-induced hypertension, including job strain-induced workplace hypertension. Workplace hypertension is prevalent; ~ 23% of public officials in the Tokyo Metropolitan Government Office (mean age, ~ 41.4 years) exhibited workplace hypertension [48] and job strain is one of most important risk factors of cardiac hypertorophy as well as hypertension [49]. Our model can provide insights to the mechanism of workplace hypertension. The circadian change of SOCE-induced NO release may contribute to the difference of the effect of STIM1 ablation on BP in the daytime and in the nighttime, in addition to the enhanced reactivity to the sympathetic tone, previously described.

In conclusion, we have found that endothelial STIM1 is a novel BP modulator via SOCE-mediated NO production. Like downregulated endothelial STIM1 expression in diabetic mice [28], STIM1 expression in ECs can be associated with pathogenesis and progression of hypertension, leading to cardiovascular diseases. Further studies are needed to clarify how STIM1 contributes to the progression of vascular diseases.

Acknowledgements We thank Ms. E. Suemune, Ms. S Kawai, and Ms. M Miyazawa for their technical assistance. We are grateful to Dr. M Sato (the University of Tokyo, Tokyo, Japan) for providing Piccell and also Dr. A Mutoh, Dr. T Marumo, Dr. W Kawarazaki, Dr. S Mu, Dr. N Ayuzawa, Dr. K Ueda, Dr. D Hirohama, and Dr. A Watanabe for their useful advice and discussion.

Funding This work was supported in part by grants from the JSPS KAKENHI [Grant Number 26860547]; Charitable Trust Araki Medical and Biochemical Research Memorial Fund; Japan Foundation for Applied Enzymology; Research Foundation for Community Medicine; and the SENSHIN Medical Research Foundation. We thank Takeda Pharmaceutical Co. Ltd.; and Novartis Pharma KK for their financial support.

Compliance with ethical standards

Conflict of interest The authors declare that they have no conflict of interest.

References

1. Perry IJ, Beevers DG. Salt intake and stroke: a possible direct effect. J Hum Hypertens. 1992;6:23–25.
2. Linder L, Kiowski W, Bühler FR, Lüscher TF. Indirect evidence for release of endothelium-derived relaxing factor in human forearm circulation in vivo. Blunted response in essential hypertension. Circulation. 1990;81:1762–7.
3. Panza JA, Quyyumi AA, Brush JE, Epstein SE. Abnormal endothelium-dependent vascular relaxation in patients with essential hypertension. N Engl J Med. 1990;323:22–27.
4. Drexler H. Factors involved in the maintenance of endothelial function. Am J Cardiol. 1998;82:3S–4S.
5. Vane JR, Anggård EE, Botting RM. Regulatory functions of the vascular endothelium. N Engl J Med. 1990;323:27–36.
6. Palmer RM, Ashton DS, Moncada S. Vascular endothelial cells synthesize nitric oxide from L-arginine. Nature. 1988;333:664–6.
7. Huang PL, Huang Z, Mashimo H, Bloch KD, Moskowitz MA, Bevan JA, Fishman MC. Hypertension in mice lacking the gene for endothelial nitric oxide synthase. Nature. 1995;377:239–42.
8. Lahera V, Salom MG, Miranda-Guardiola F, Moncada S, Romero JC. Effects of NG-nitro-L-arginine methyl ester on renal function and blood pressure. Am J Physiol. 1991;261:F1033–7.
9. Leonard AM, Chafe LL, Montani J-P, Van Vliet BN. Increased salt-sensitivity in endothelial nitric oxide synthase-knockout mice. Am J Hypertens. 2006;19:1264–9.
10. Sessa WC. eNOS at a glance. J Cell Sci. 2004;117:2427–9.
11. Dudzinski DM, Michel T. Life history of eNOS: partners and pathways. Cardiovasc Res. 2007;75:247–60.
12. Lewis RS. The molecular choreography of a store-operated calcium channel. Nature. 2007;446:284–7.
13. Lin S, Fagan KA, Li KX, Shaul PW, Cooper DM, Rodman DM. Sustained endothelial nitric-oxide synthase activation requires capacitative Ca^{2+} entry. J Biol Chem. 2000;275:17979–85.
14. Dimmeler S, Fleming I, Fisslthaler B, Hermann C, Busse R, Zeiher AM. Activation of nitric oxide synthase in endothelial cells by Akt-dependent phosphorylation. Nature. 1999;399:601–5.
15. Hartmannsgruber V, Heyken W-T, Kacik M, Kaistha A, Grgic I, Harteneck C, Liedtke W, Hoyer J, Köhler R. Arterial response to shear stress critically depends on endothelial TRPV4 expression. PLoS ONE. 2007;2:e827.
16. Wang S, Iring A, Strilic B, Albarrán Juárez J, Kaur H, Troidl K, Tonack S, Burbiel JC, Müller CE, Fleming I, Lundberg JO, Wettschureck N, Offermanns S. $P2Y_2$ and Gq/G_{11} control blood pressure by mediating endothelial mechanotransduction. J Clin Invest. 2015;125:3077–86.
17. Jung B, Obinata H, Galvani S, Mendelson K, Ding B-S, Skoura A, Kinzel B, Brinkmann V, Rafii S, Evans T, Hla T. Flow-regulated endothelial S1P receptor-1 signaling sustains vascular development. Dev Cell. 2012;23:600–10.
18. Zhang SL, Yu Y, Roos J, Kozak JA, Deerinck TJ, Ellisman MH, Stauderman KA, Cahalan MD. STIM1 is a Ca^{2+} sensor that activates CRAC channels and migrates from the Ca^{2+} store to the plasma membrane. Nature. 2005;437:902–5.
19. Williams RT, Manji SS, Parker NJ, Hancock MS, Van Stekelenburg L, Eid JP, Senior PV, Kazenwadel JS, Shandala T, Saint R, Smith PJ, Dziadek MA. Identification and characterization of the STIM (stromal interaction molecule) gene family: coding for a novel class of transmembrane proteins. Biochem J. 2001;357:673–85.
20. Brandman O. STIM2 is a feedback regulator that stabilizes basal cytosolic and endoplasmic reticulum Ca^{2+} levels. Cell. 2007;131:1327–39.
21. Zhou Y, Mancarella S, Wang Y, Yue C, Ritchie M, Gill DL, Soboloff J. The short N-terminal domains of STIM1 and STIM2 control the activation kinetics of Orai1 channels. J Biol Chem. 2009;284:19164–8.
22. Baba A, Yasui T, Fujisawa S, Yamada RX, Yamada MK, Nishiyama N, Matsuki N, Ikegaya Y. Activity-evoked capacitative Ca^{2+} entry: implications in synaptic plasticity. J Neurosci. 2003;23:7737–41.
23. Berna Erro A, Braun A, Kraft R, Kleinschnitz C, Schuhmann MK, Stegner D, Wultsch T, Eilers J, Meuth SG, Stoll G, Nieswandt B. STIM2 regulates capacitive Ca^{2+} entry in neurons and plays a key role in hypoxic neuronal cell death. Sci Signal. 2009;2:ra67–ra67.
24. Ma J, McCarl C-A, Khalil S, Lüthy K, Feske S. T-cell-specific deletion of STIM1 and STIM2 protects mice from EAE by impairing the effector functions of Th1 and Th17 cells. Eur J Immunol. 2010;40:3028–42.
25. Abdullaev IF, Bisaillon JM, Potier M, Gonzalez JC, Motiani RK, Trebak M. Stim1 and Orai1 mediate CRAC currents and store-operated calcium entry important for endothelial cell proliferation. Circ Res. 2008;103:1289–99.
26. Hirano K, Hirano M, Hanada A. Involvement of STIM1 in the proteinase-activated receptor 1-mediated Ca^{2+} influx in vascular endothelial cells. J Cell Biochem. 2009;108:499–507.
27. Gandhirajan RK, Meng S, Chandramoorthy HC, Mallilankaraman K, Mancarella S, Gao H, Razmpour R, Yang X-F, Houser SR, Chen J, Koch WJ, Wang H, Soboloff J, Gill DL, Madesh M. Blockade of NOX2 and STIM1 signaling limits lipopolysaccharide-induced vascular inflammation. J Clin Invest. 2013;123:887–902.
28. Estrada IA, Donthamsetty R, Debski P, Zhou M-H, Zhang SL, Yuan JX-J, Han W, Makino A. STIM1 restores coronary endothelial function in type 1 diabetic mice. Circ Res. 2012;111:1166–75.
29. Kassan M, Zhang W, Aissa KA, Stolwijk J, Trebak M, Matrougui K. Differential role for stromal interacting molecule 1 in the regulation of vascular function. Pflug Arch. 2015;467:1195–202.
30. Kisanuki YY, Hammer RE, Miyazaki J, Williams SC, Richardson JA, Yanagisawa M. Tie2-Cre transgenic mice: a new model for endothelial cell-lineage analysis in vivo. Dev Biol. 2001;230:230–42.
31. Kobayashi M, Inoue K, Warabi E, Minami T, Kodama T. A simple method of isolating mouse aortic endothelial cells. J Atheroscler Thromb. 2005;12:138–42.
32. Mutoh A, Isshiki M, Fujita T. Aldosterone enhances ligand-stimulated nitric oxide production in endothelial cells. Hypertens Res. 2008;31:1811–20.
33. Sato M, Nakajima T, Goto M, Umezawa Y. Cell-based indicator to visualize picomolar dynamics of nitric oxide release from living cells. Anal Chem. 2006;78:8175–82.
34. Mu S, Shimosawa T, Ogura S, Wang H, Uetake Y, Kawakami-Mori F, Marumo T, Yatomi Y, Geller DS, Tanaka H, Fujita T. Epigenetic modulation of the renal β-adrenergic-WNK4 pathway in salt-sensitive hypertension. Nat Med. 2011;17:573–80.
35. Oh-hora M, Yamashita M, Hogan PG, Sharma S, Lamperti E, Chung W, Prakriya M, Feske S, Rao A. Dual functions for the endoplasmic reticulum calcium sensors STIM1 and STIM2 in T cell activation and tolerance. Nat Immunol. 2008;9:432–43.
36. Mancarella S, Potireddy S, Wang Y, Gao H, Gandhirajan RK, Autieri M, Scalia R, Cheng Z, Wang H, Madesh M, Houser SR, Gill DL. Targeted STIM deletion impairs calcium homeostasis, NFAT activation, and growth of smooth muscle. FASEB J. 2013;27:893–906.
37. Chataigneau T, Félétou M, Huang PL, Fishman MC, Duhault J, Vanhoutte PM. Acetylcholine-induced relaxation in blood vessels

from endothelial nitric oxide synthase knockout mice. Br J Pharmacol. 1999;126:219–26.
38. Isshiki M, Mutoh A, Fujita T. Subcortical Ca^{2+} waves sneaking under the plasma membrane in endothelial cells. Circ Res. 2004;95:e11–21.
39. Devereux RB, Pickering TG, Alderman MH, Chien S, Borer JS, Laragh JH. Left ventricular hypertrophy in hypertension. Prevalence and relationship to pathophysiologic variables. Hypertension. 1987;9:II53–60.
40. Colhoun HM, Dong W, Poulter NR. Blood pressure screening, management and control in England: results from the health survey for England 1994. J Hypertens. 1998;16:747–52.
41. Franklin SS, Jacobs MJ, Wong ND, L'Italien GJ, Lapuerta P. Predominance of isolated systolic hypertension among middle-aged and elderly US hypertensives: analysis based on National Health and Nutrition Examination Survey (NHANES) III. Hypertension. 2001;37:869–74.
42. Chirinos JA, Franklin SS, Townsend RR, Raij L. Body mass index and hypertension hemodynamic subtypes in the adult US population. Arch Intern Med. 2009;169:580–6.
43. Baguet J-P, Hammer L, Lévy P, Pierre H, Rossini E, Mouret S, Ormezzano O, Mallion J-M, Pépin J-L. Night-time and diastolic hypertension are common and underestimated conditions in newly diagnosed apnoeic patients. J Hypertens. 2005;23:521–7.
44. Verdecchia P, Angeli F. Natural history of hypertension subtypes. Circulation. 2005;111:1094–6.
45. McEniery CM, Yasmin, Wallace S, Maki-Petaja K, McDonnell B, Sharman JE, Retallick C, Franklin SS, Brown MJ, Lloyd RC, Cockcroft JR, Wilkinson IB. ENIGMA Study Investigators. Increased stroke volume and aortic stiffness contribute to isolated systolic hypertension in young adults. Hypertension. 2005;46:221–6.
46. Ortiz PA, Garvin JL. Role of nitric oxide in the regulation of nephron transport. Am J Physiol Ren Physiol. 2002;282:F777–84.
47. Kopkan L, Hess A, Husková Z, Cervenka L, Navar LG, Majid DSA. High-salt intake enhances superoxide activity in eNOS knockout mice leading to the development of salt sensitivity. Am J Physiol Ren Physiol. 2010;299:F656–63.
48. Harada K, Karube Y, Saruhara H, Takeda K, Kuwajima I. Workplace hypertension is associated with obesity and family history of hypertension. Hypertens Res. 2006;29:969–76.
49. Schnall PL, Pieper C, Schwartz JE, Karasek RA, Schlussel Y, Devereux RB, Ganau A, Alderman M, Warren K, Pickering TG. The relationship between 'job strain,' workplace diastolic blood pressure, and left ventricular mass index. Results of a case-control study. JAMA. 1990;263:1929–35.